Q. J. R. Meteorol. Soc. (1994), **120**, pp. 573–601 551.574.13:551.576.11

Ice particle concentrations and precipitation development in small continental cumuliform clouds

By ARTHUR L. RANGNO and PETER V. HOBBS*
University of Washington, USA

(Received 21 January 1993; revised 28 September 1993)

SUMMARY

Maximum ice particle concentrations (I_M) in modest ($\leq$3.7 km deep) continental cumuliform clouds, with tops with temperatures between −6 and −25 °C, were found to be better correlated with the broadness of the droplet spectrum near cloud top ($r = 0.78$) than with cloud-top temperature ($r = 0.58$). Also, the broader the droplet spectrum the warmer was the cloud top at which ice first appeared.

Stratification into three cloud-base-temperature (T_B) categories, cool ($0\,°C \leq T_B \leq 8\,°C$), cold ($-8\,°C < T_B < 0\,°C$), and very cold ($T_B \leq -8\,°C$), produced correlations between I_M and cloud-top temperature (T_T) of 0.71, 0.88, and 0.89, respectively. The best-fit lines for these relationships shift to higher I_M values as T_B increases; this also reflects the effect on I_M of the broadness of the droplet spectrum, since the size of the largest drops increases as T_B increases. When the clouds contained drops with diameters $\geq$25 μm, ice particle formation was sudden and prolific. High concentrations of ice particles appeared coincident with, or very soon after, the formation of graupel; these high concentrations were observed in clouds at ambient temperatures between −11 and −28 °C, including some clouds with $T_B < 0\,°C$.

For clouds with similar droplet spectra and T_T, the width of the cloud also affected I_M; narrow clouds (<2 km wide) formed less ice than wider, multi-turreted clouds.

Continental cumulus clouds have to be about 50% wider and about 5 degC colder at their tops than maritime cumulus to have the same chance of producing a radar echo. However, the difference in width to produce a radar echo disappears for clouds with widths >4 km, although continental clouds still need to be about 5 degC colder at cloud top than maritime clouds to produce a radar echo.

Several extant theories for high ice particle concentrations in clouds are examined but none provides a satisfactory explanation for the observations.

1. INTRODUCTION

In previous papers we have reported on ice particle concentrations and precipitation development in maritime cumuliform clouds (Hobbs and Rangno 1985, 1990a; Rangno and Hobbs 1991). In this paper we discuss the same topic but for continental cumuliform clouds. The expression 'cumuliform clouds' includes cumulus (e.g. humilis, mediocris, etc.), cumulonimbus (e.g. capillatus, calvus, etc.) and stratocumulus clouds.

The results reported here are based on airborne measurements in 575 clouds, principally continental cumuliform clouds that formed over and east of the Cascade Mountains in Washington State (Hobbs and Rangno 1992). They cover a wide range of cloud-base temperatures (−18 to 8 °C), cloud-droplet concentrations (300 to ~1500 cm^{-3}) and cloud-droplet spectra. Cloud-top temperatures ranged from −5.5 to −32.5 °C.

The clouds formed in modified polar maritime air, and in air carried many thousands of kilometres from tropical latitudes. The clouds were modest in vertical extent ($\leq$3.7 km thick), with updraughts <5 m s^{-1}. Since we generally chose days with stable layers aloft, as the rising cumulus turrets approached their maximum height they were generally colder than the ambient air.

In addition to the data collected over and east of the Cascade Range, data from three other flights are included in this study. One of these (3 February 1989) was in shallow cumulus and stratocumulus clouds near the coast of Washington State in extremely cold continental arctic air. The second (4 March 1990) was in several cumulus congestus

* Corresponding author: Atmospheric Sciences Department, University of Washington, Seattle, Washington, USA.

clouds over the Puget Sound of Washington State in light offshore winds. The third (12 March 1992) was in small but cold postfrontal cumulus and stratocumulus clouds over Kansas.

2. Instrumentation and methods of analysis

The aircraft sampling methods and instrumentation used in this study have been described by Rangno and Hobbs (1991). With one exception the methods used to analyse the data are also the same as those described by Rangno and Hobbs (1991). The exception is the computation of the total concentrations of droplets with diameters $\geqslant 20\ \mu m$ and $\geqslant 23\ \mu m$. Rangno and Hobbs considered the cumulative concentrations of droplets counted in and above channels 7 and 8 of the Particle Measuring Systems (PMS) Model-100 Forward Scattering Spectrometer Probe (FSSP) to be the concentrations of droplets with diameters $\geqslant 20\ \mu m$ and $\geqslant 23\ \mu m$ diameter, respectively. To ensure that the concentrations of larger droplets are not under-represented by the FSSP measurements (see Baumgardner and Spowart 1990) we now average the cumulative concentrations indicated in channels 6 and 7 to represent the concentration of droplets $\geqslant 20\ \mu m$ diameter (this increases the derived concentrations of droplets with diameter $\geqslant 20\ \mu m$). Similarly, the cumulative concentrations of droplets equal to and larger than those measured in FSSP channels 7 and 8 have been averaged and assigned to channel 8; this raises the derived concentrations of droplets with diameter $\geqslant 23\ \mu m$. These adjustments are compatible with our assumption that the FSSP size range extends to 48–51 μm in channel 15, rather than to 44–47 μm size (which is what PMS states). The latter adjustment produces closer agreement between the liquid-water contents derived from the FSSP and those measured simultaneously by the Johnson–Williams (J–W) and King liquid-water probes. The droplet parameter, D_T, which provides a measure of the broadness of the droplet spectrum, is the droplet diameter for which the cumulative total of larger drops is $3\ cm^{-3}$, as measured in regions where the liquid-water content (measured by the J–W probe) is $\geqslant 0.3\ gm^{-3}$ and the ice particle concentration is $<1\ L^{-1}$. The latter criterion virtually eliminated any artificial broadening of the droplet spectra measured by the FSSP due to ice particles.

The maximum ice particle concentrations (I_M) for particles $\geqslant 100\ \mu m$ in maximum dimension were calculated from the PMS 2-D cloud probe by dividing the greatest number of accepted particles (see Rangno and Hobbs 1991) measured over path lengths of 250–300 m by the air volumes sampled. Since the two-dimensional (2-D) precipitation probe samples about 17 times more volume in air in every second than does the 2-D cloud probe, when ice particles concentrations were very low ($<0.3\ L^{-1}$) their concentrations were measured using the PMS 2-D precipitation probe. The highest concentrations of ice particles in cumuliform clouds were almost always measured in mature or aging clouds with widths $\geqslant 2$ km when sampled $\geqslant 50$ m below cloud top. These maximum ice particle concentrations are considerably lower than the actual maximum ice particle concentrations by at least 50% for the reasons mentioned by Rangno and Hobbs (1991), and because a comparison of the earlier manufactured 2-D cloud probes, such as ours, with the latest probes with enhanced electronics, has shown that the newer probes image about 50% more particles (Gayet *et al.* 1993).

The cloud-top temperature at which ice first appeared in concentrations of about $1\ L^{-1}$ on each flight day (usually involving several dozen cloud penetrations) was determined in the following way. On a cloud-top temperature versus maximum ice particle concentration diagram, a straight line was fitted between clouds with the highest cloud-top temperature in which ice particle concentrations were detected (usually $\geqslant 1\ L^{-1}$) and

the cloud with the lowest cloud-top temperature in which no ice particles were found in it, or any cloud with a warmer top. The point at which this line intersected an ice particle concentration of $1\ L^{-1}$ was taken to be the temperature for ice onset for that day.

Aircraft-produced ice particles (called APIPs by Rangno and Hobbs (1983, 1984)) were measured on 32 occasions during this airborne programme. This is a far higher incidence than we encountered in our studies of maritime clouds (Rangno and Hobbs 1991). This can be attributed to the lower in-cloud temperatures (by 8 degC on average) in the present study. We used the same techniques in this paper to eliminate APIPs in the data analysis as those described by Rangno and Hobbs (1991).

The data were partitioned according to the stage (young, mature, and dissipating) in the life cycle of the cloud at which they were collected. In addition to those factors used by Rangno and Hobbs (1991) to determine the stage in the life cycle, the mean droplet concentration in the cloud was used. A droplet concentration above the mean for a particular day was considered to be an indicator of rising air, and therefore of younger clouds (e.g. Rogers *et al.* 1985; Politovich and Cooper 1988). Ragged, evaporating cloud turrets at the end of their life cycle have lower average droplet concentrations, lower liquid-water contents, and frequently contain regions of clear air (e.g. Schemenauer and Isaac 1984). Thus droplet concentrations below the mean were used to help flag dissipating clouds. Also, the youngest, firmest looking cloud turrets, nearing the maximum height of the clouds on a particular day, were always colder than their environment (frequently by more than 2 degC). The temperatures of dissipating, stratiform cloud remnants, on the other hand, differed little from that of the ambient air. Hence, in-cloud temperatures, obtained in the uppermost cloud regions, that were lower than ambient temperatures were also a sign of a newly risen (and about to sink) cloud turret.

Cloud-top height and width for most clouds were derived from triangulation, using the images from the forward-pointing video camera mounted on the aircraft. In many cases cloud-top heights and widths were measured directly from the aircraft.

3. Overview of results[1]

(*a*) *Ice-nucleus measurements*

Ice-nucleus measurements obtained with Millipore filters during the flights have been discussed by Rosinski (1991). When the filters were analysed in the usual way (by exposing them to water saturations at a fixed temperature), the measured ice-nucleus concentrations were similar to those summarized by Fletcher (1962). However, when the filters were subjected to a cycle of condensation and evaporation, or to supersaturations with respect to water, considerably higher concentrations of ice nuclei than those given by Fletcher were measured above $-17\,°C$. For example, in continental air over eastern Washington, about $2–4\ L^{-1}$ of ice nuclei active at $-15\,°C$ were measured in the first condensation–evaporation cycle. This is almost a factor of 20–30 greater than the concentrations predicted by Fletcher's curve, but it is consistent with more recent measurements of ice-nucleus concentrations summarized by Meyers *et al.* (1992).

(*b*) *The onset of ice in continental cumuliform clouds*

When the concentration of ice in a cumuliform cloud reaches about $1\ L^{-1}$ it can produce significant precipitation through ice-crystal growth. Therefore, we refer to this concentration as the *onset* of ice. Our measurements show that the onset of ice near

[1] A complete tabulation of the present data set for continental cumuliform clouds (and our earlier data set for maritime cumuliform clouds) may be obtained from the authors.

cloud top can be predicted for continental cumulus clouds from their cloud-base temperature (T_B). Figure 1(a) shows that the cloud-top temperature (T_T) (accurate to about ±1.5 degC) for the onset of ice in concentrations of 1 L^{-1} is well correlated with T_B (r = 0.91); the warmer the cloud base, the higher is the T_T at which ice first appears. For comparison, the line derived by Rangno and Hobbs (1988) from an analysis of many other cloud studies around the world is also shown in Fig. 1(a), where it can be seen to be very similar to the present results. The line shown in Fig. 1(a) is represented by:

$$T_T = 0.4T_B - 13.5 \quad (1)$$

where the temperatures are in degrees Celsius. Since T_T and T_B are often estimated in numerical models, (1) provides a useful relation for use in such models for determining whether or not an ice concentration of 1 L^{-1} is likely to be attained in a cumuliform cloud. T_T for the onset of ice can also be related to the cloud depth, D (km), by Fig. 1(b):

$$T_T = 4.5 \ln D - 16. \quad (2)$$

Both T_B and D are surrogates for the broadness of the droplet size distribution at cloud top. Following Hobbs and Rangno (1985) the broadness of the droplet size distribution can be represented by the *droplet threshold diameter* (D_T), which is defined as the droplet diameter for which the total concentration of droplets with diameters $\geq D_T$ is 3 cm^{-3} (as measured by the FSSP). Figure 1(c) shows T_T for ice onset versus D_T (r = 0.80). These measurements show that increasingly large cloud droplets are required for the initiation of ice as the cloud-top temperature increases. To illustrate further the essential role of the broadness of the droplet spectrum in determining the onset of ice, we have added to Fig. 1(c) the results from our study of maritime cumuliform clouds (Hobbs and Rangno 1990b). For the combined continental and maritime data sets, the correlation coefficient between T_T and D_T is r = 0.88. The empirical relation between T_T (°C) for ice onset and D_T (μm) is from the line in Fig. 1(c):

$$T_T = 0.6\, D_T - 28. \quad (3)$$

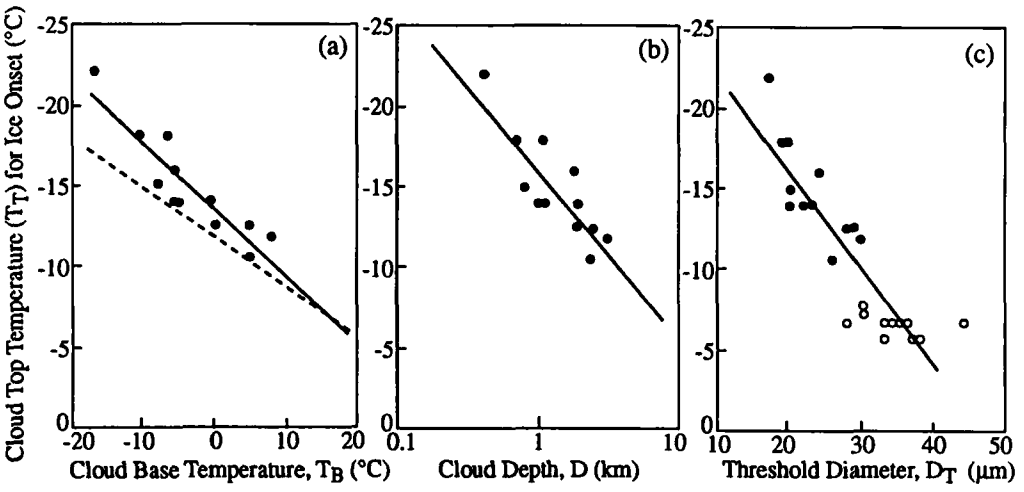

Figure 1. The onset of ice in continental cumuliform clouds (filled circles) as a function of (a) cloud-base temperature, (b) cloud depth, and (c) droplet threshold diameter. The solid lines are the best-fit lines to the present data set. The dashed line in (a) is that deduced by Rangno and Hobbs (1988) from a review of many studies worldwide. The Hobbs and Rangno (1990b) data for maritime cumuliform clouds are shown in (c) by the open circles.

Figure 2 shows the percentage chance of intercepting any ice particles in aging cumuliform clouds. Four techniques were used for detecting the presence of ice particles: the University of Washington (UW) Optical Ice Particle Counter (Turner *et al.* 1976), the PMS 2-D cloud and precipitation probes, ice crystal replicas on glass slides, and the UW airborne 35 GHz radar. (Owing to the near absence of drizzle or raindrops during the sampling programme, a radar echo was attributed to ice particles.) It can be seen from Fig. 2 that regardless of cloud-base temperatures the chance of detecting ice particles in an aging cumuliform cloud increases as the cloud-top temperature decreases; the chance of intercepting ice particles is near 100 per cent for aging cumuliform clouds with tops colder than about −12 °C.

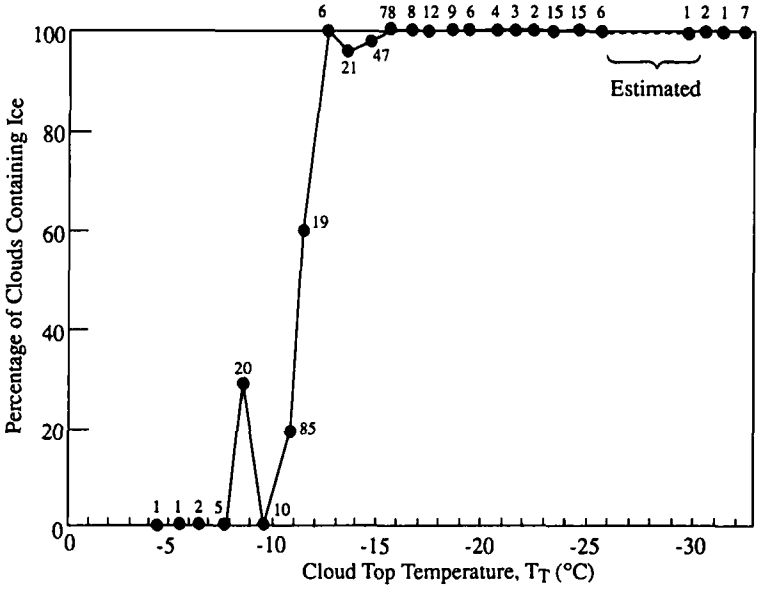

Figure 2. The percentage chance of intercepting ice particles in concentrations $\geq 1\ L^{-1}$ in aging or dissipating continental cumuliform clouds of all widths based on data from the present study. The number alongside each point is the total number of clouds sampled.

(*c*) *Effect of the life cycle of cumuliform clouds on the concentrations of ice particles*

Figure 3 shows I_M very near, and well below, cloud top as a function of T_T for newly risen and aging cumuliform clouds. If $T_B \geq 0$ °C the onset of ice in aging continental cumuliform clouds occurs at $T_T = -11 \pm 3$ degC (see Fig. 1(a)). The highest ice particle concentrations are generally found in aging clouds at distances ≥50 m below their tops (compare Fig. 3(b) with Fig. 3(d)). This may be due to the settling to these levels of ice particles large enough to be detected (≥100 μm diameter); the uppermost cloud regions probably contained ice particles <100 μm diameter, which could not be measured. The concentrations of ice particles continue to increase as T_T decreases and, correspondingly, cloud depth increases. The measured sizes of the ice particles suggests that the time required to produce the maximum concentrations of ice in a cloud is ≤10 min from the time the cloud top approaches its maximum height.

(*d*) *Locations of the origins of the ice particles*

The sizes and habits of ice particles collected in the clouds were studied, using PMS 2-D imagery and Formvar replicas of ice crystals, to determine how far they had been

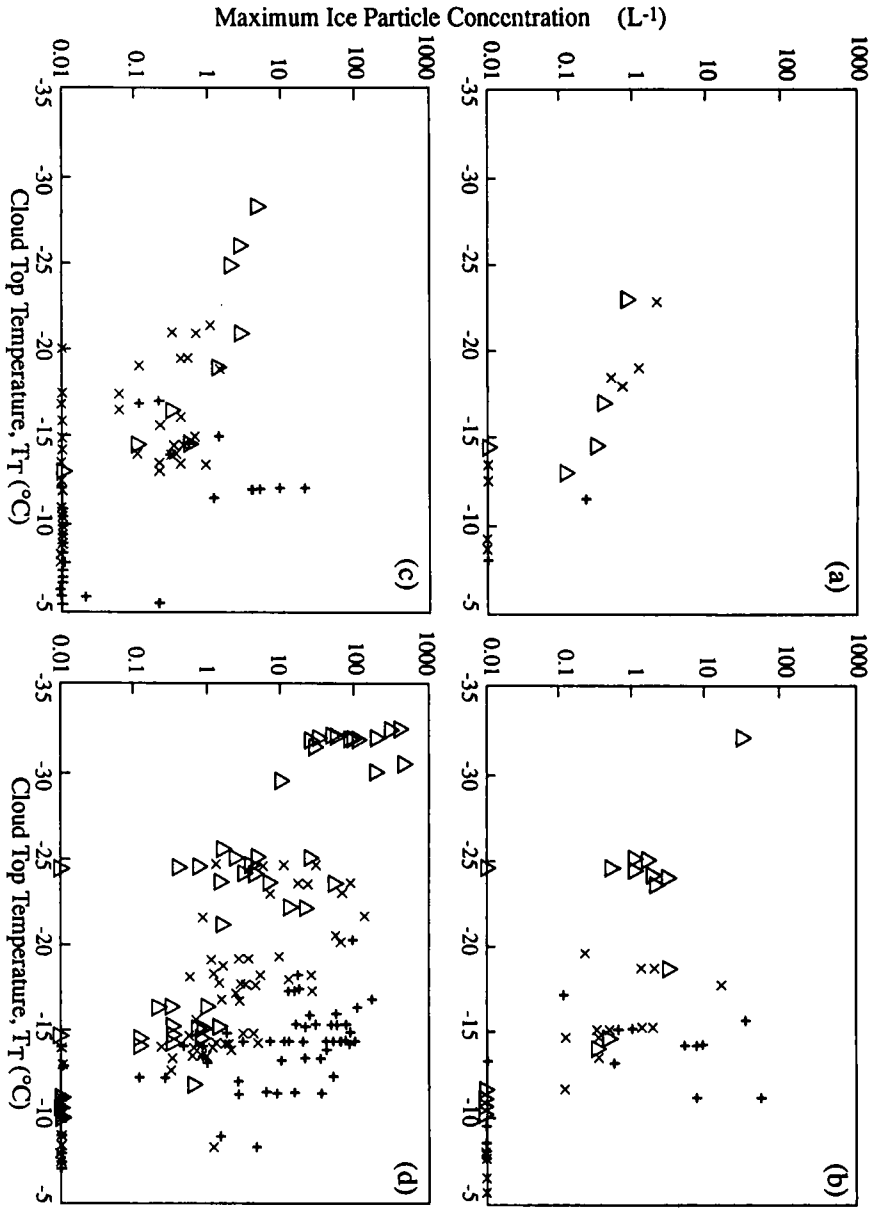

Figure 3. Maximum ice particle concentrations in continental cumuliform clouds: (a) <50 m below the tops of young clouds; (b) <50 m below the tops of aging, dissipating clouds; (c) ≥50 m below the tops of young, rising clouds; and (d) ≥50 m below the tops of aging, dissipating clouds. The triangles are for clouds with base temperatures (T_B) ≤ −8 °C, the crosses for −8 °C < T_B < 0 °C, and the plus signs for 0 °C ≤ T_B ≤ 8 °C.

transported from their temperature zones of formation. Crystals were assumed to have been transported in the vertical if they were encountered more than 1 degC from their temperature zone of formation. For example, if columnar ice crystals (e.g. hollow columns, sheaths and needles) were encountered at < -11 °C they were assumed to have been transported, since these types of columnar ice crystals form at temperatures no lower than -10 °C in a water saturated environment (e.g. Mason 1971).

A total of 870 PMS 2-D image 'periods' (during a period there were no significant changes in ice particle habits or concentrations) were examined. Only 14 periods, or 2% of the total imagery, all of which occurred on the same day (18 May 1989), contained some ice crystals that had been transported *upward* from their temperature zone of formation. On the other hand 38% of the periods contained some ice particles that had been transported or fallen from regions *above* the aircraft flight level. The crystal habits in the remaining 60% of the periods were compatible with having formed very close to where they were collected. Since the assignment of crystal habits from 2-D imagery can be imprecise owing to relatively low resolution for small particles, we will now discuss ice particle replicas obtained on Formvar-coated microscope slides exposed in the clouds. These replicas provide more detail on ice crystal forms.

Tabulations of ice crystal type by flight-level temperature were made for all cases where cloud temperatures permitted unambiguous determination of the level of origin of the crystals (in some cases this is not possible owing to certain crystal habits forming in more than one temperature zone). This analysis focused on hollow columnar crystals, sector plates and stellars, and dendritic fragments. Of the 112 (decipherable) slides exposed in clouds only about 10% of all the slides contained ice particles that had been transported from below, and these were all on the same day (18 May 1989) when plates were replicated in vigorous cumuliform clouds at temperatures between -22 and -29 °C. Ninety per cent of the ice crystal replicas on the Formvar were of ice particles that fell from above the flight level, or formed at the temperature at which they were intercepted. This indicates that the ice particles either formed near the end of the updraught cycle, where upward transport would have been unlikely, or the ice crystals settled out in downdraughts.

(*e*) *Rapid formation of ice particles*

In clouds with $T_T \leqslant -15$ °C, but with a relatively narrow droplet spectrum (D_T between 15 and 20 μm diameter) near cloud top, relatively few ice particles formed and the size spectrum of the ice particles was broad, indicating that, rather than forming suddenly, the ice particles formed over a period of time by a 'trickle' mechanism. When larger droplets ($D_T \geqslant 25$ μm diameter) were plentiful in the upper regions of young cumuliform clouds, high concentrations (tens to hundreds per litre) of relatively uniform sized, and apparently vapour-grown, ice crystals appeared coincident with, or perhaps shortly after, the formation of graupel particles. These ice particles were nearly always compatible in habit with the temperature at which they were collected. Such events were encountered from -10 to -28 °C, which spans several ice crystal habit regimes. However, unlike the maritime clouds studied by Hobbs and Rangno (1990a) and Rangno and Hobbs (1991), rarely did these events involve columnar ice particles. This is probably because in these relatively cool clouds large droplets did not develop until the turrets had reached a level where their temperature was -10 °C or lower. Figures 4(a) and (b) show two such occurrences. The high concentrations of small, uniform-sized ice crystals depicted in Figs. 4(a) and (b) show a striking resemblance to the uniformly sized ice crystals that form in clouds seeded with dry ice (Fig. 4(c)).

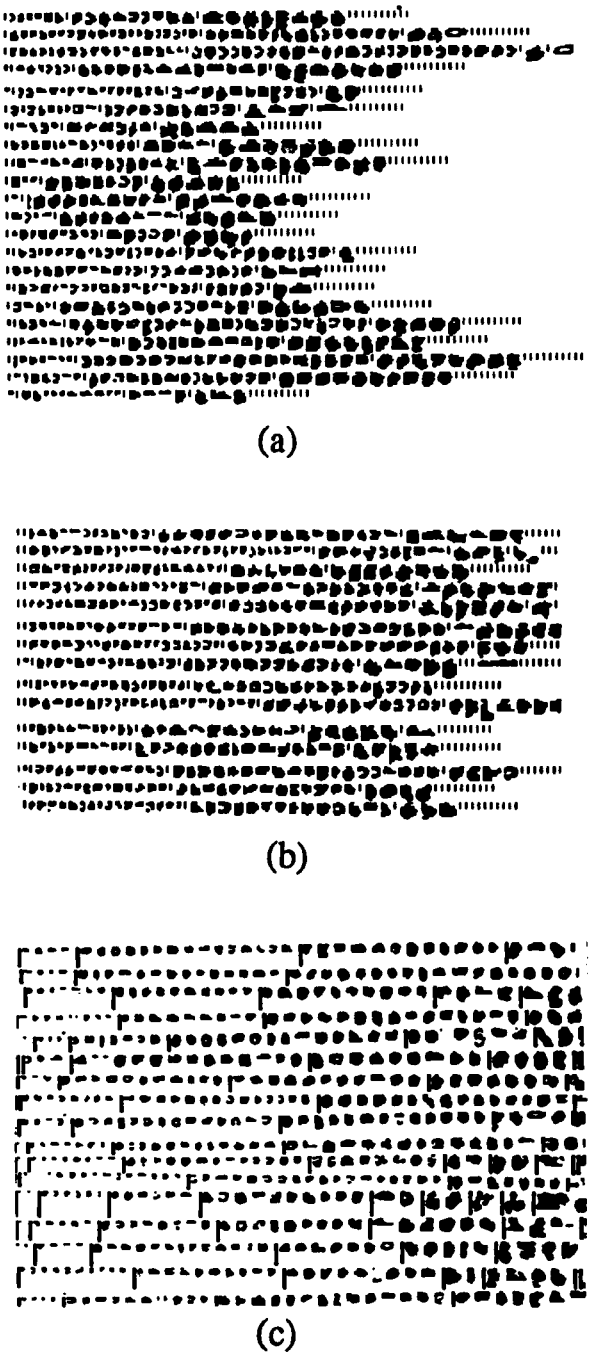

Figure 4. Examples of contiguous PMS 2-D cloud probe imagery showing high concentrations of uniformly sized ice particles encountered in natural cumuliform continental clouds at (a) −25 °C and (b) −11 °C (graupel particles are not shown). For comparison the ice particles imaged in a cloud seeded with dry ice at −10 °C are shown in (c). The particles have been arranged in order of increasing size.

(f) The effect of cloud width on ice particle concentrations in aging clouds

Figure 5 shows that the maximum concentrations of ice particles, I_M, in mature and aging continental cumuliform clouds increase as the cloud width, W, in their upper regions increases. The empirical relation between I_M (L^{-1}) and W (km) from Fig. 5 is:

$$I_M = \left(\frac{W}{1.8}\right)^{1.6}. \tag{4}$$

Moderately supercooled and narrow (<2 km wide) clouds with subsiding tops were rarely observed to produce maximum ice particle concentrations in excess of $10\,L^{-1}$.

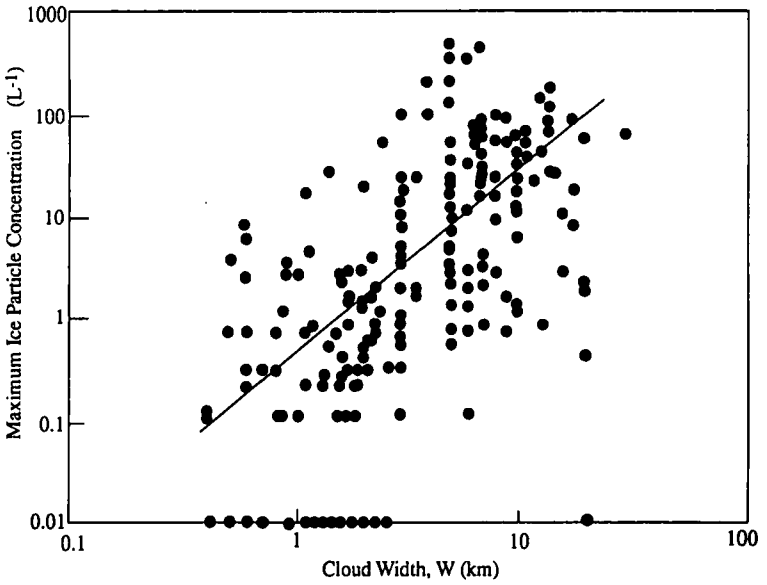

Figure 5. Maximum ice particle concentrations in aging clouds versus width of cloud for continental cumuliform clouds sampled in their upper regions. The best-fit line to the data is shown.

(g) Radar echo widths

Figure 6 shows the frequency of detection of 35 GHz radar echoes of various widths in continental cumuliform clouds. The radar was mounted on the aircraft and was generally pointed downward while the aircraft was flying in the upper half of the clouds. The results are similar to those reported by Rangno and Hobbs (1991) for maritime clouds, which are also shown in Fig. 6. However, there are two important differences. The continental cumuliform clouds had to be, on average, 50% or more wider in their upper regions than the maritime clouds, and about 5 degC colder, to have a 95% chance of producing a measurable radar echo. The tops of the maritime cumuliform clouds had to reach −7 °C to have a 95% chance of producing a radar echo. In continental clouds, irrespective of other conditions, the cloud-top temperature had to be ≤−12.5 °C before there was at least a 95% chance of producing a radar echo. Also, the modal radar echo width is shifted from 2 km in the maritime clouds to 3 km in the continental clouds. These measurements support a remarkable speculation of Findeisen (1942, see Mossop 1985a) that maritime and continental cumuliform clouds have about the same chance of producing precipitation if the continental clouds have top temperatures about 5 degC cooler

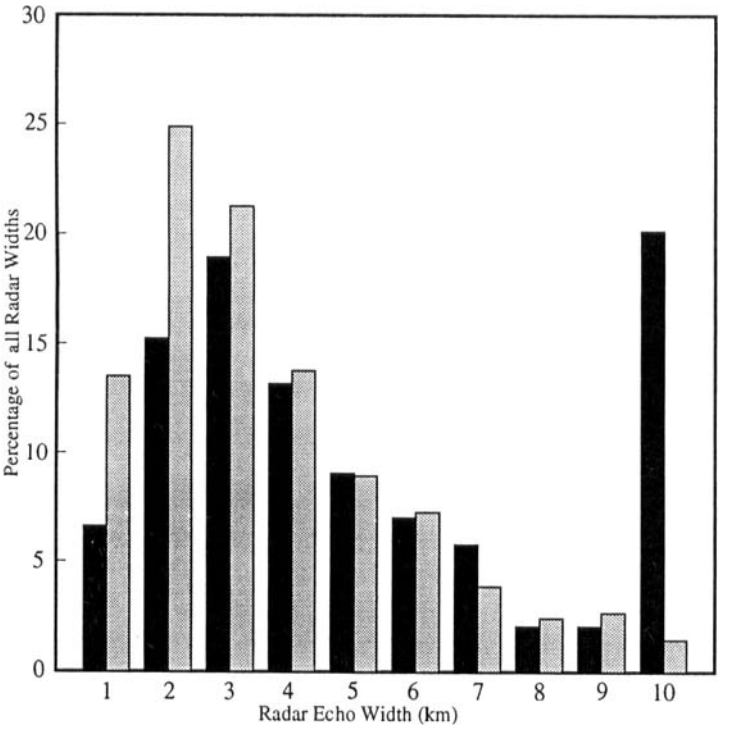

Figure 6. Histogram of frequency of occurrence of radar echo widths in small continental cumuliform clouds (solid) and small maritime cumuliform clouds (stippled). The vertically pointed radar, which was mounted on the research aircraft, had a frequency of 35 GHz.

than the maritime clouds. Many of the continental clouds that were <3 km wide did not produce radar echoes, although they often had a few ice particles in them at flight level in dissipating, wispy cloud regions.

The difference between maritime and continental clouds in echo-producing frequency disappears where the width of the clouds exceeds about 4 km. Thus continental clouds that are at least 4 km wide are as likely to precipitate as maritime clouds of the same width.

(*h*) *Effect of cloud-top temperature on maximum ice particle concentrations*

Relationships between I_M and T_T for aging cumuliform clouds are shown in Fig. 7(a). For the data set as a whole there is a moderate overall logarithmic correlation ($r = 0.71$) between I_M and T_T.

It is revealing to examine the I_M–T_T relationships in sub-sets partitioned by T_B (Fig. 7(a)). For continental cumuliform clouds with $T_B < 0$ °C there is a very strong correlation between I_M and T_T. For example, for $T_B \leq -8$ °C the correlation coefficient between I_M and T_T is 0.89. For this sub-set of the data (line 1 in Fig. 7(a)) the relation between I_M (L^{-1}) and T_T (°C) is:

$$I_M = \left(\frac{T_T}{-17}\right)^{7.1}. \tag{5}$$

This is similar to Fletcher's (1962) empirical relation between measurements of atmospheric ice-nucleus concentrations and temperature.

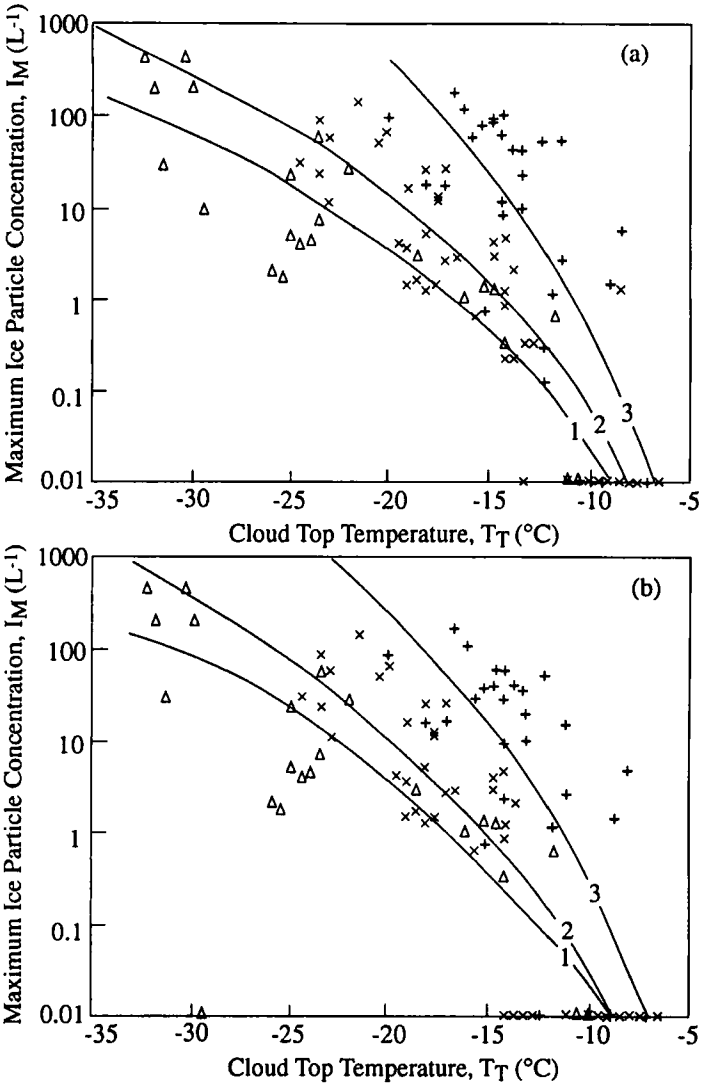

Figure 7. (a) Maximum ice particle concentration versus cloud-top temperature for aging continental cumuliform clouds for three categories of cloud-base temperature (T_B): $T_B \leq -8\,°C$ (triangles, line 1), $-8\,°C < T_B < 0\,°C$ (crosses, line 2), and $0\,°C \leq T_B \leq 8\,°C$ (plus signs, line 3). (b) Maximum concentrations of *non-columnar* ice particles, symbolia and lines are the same as in (a).

For $-8\,°C < T_B < 0\,°C$ (line 2 in Fig. 7(a)), the correlation between I_M and T_T is still very high ($r = 0.88$), but I_M is 10–50 times higher for the same T_T than for clouds with $T_B \leq 8\,°C$. The empirical relationship for line 2 in Fig. 7(a) is:

$$I_M = \left(\frac{T_T}{-14.5}\right)^{7.6}. \tag{6}$$

For $0\,°C \leq T_B \leq 8\,°C$ (line 3 in Fig. 7(a)) the correlation coefficient between I_M and T_T is 0.71, and the I_M values are 50–200 times greater for the same T_T than for clouds with $T_B \leq -8\,°C$ (and, thus, 50–200 times greater than the ice particle concentrations

that would be derived from Fletcher's relation). The empirical relationship for line 3 in Fig. 7(a) is:

$$I_M = \left(\frac{T_T}{-10.7}\right)^{9.4}. \tag{7}$$

Thus for small continental cumuliform clouds, the best-fit curves between I_M and T_T shift toward higher I_M as T_B increases. This effect is present even when the contribution of columnar ice particles to I_M is removed (Fig. 7(b)). For example, on a day with $T_B > 0$ °C, there might well be >100 L^{-1} maximum ice particle concentration in an aging cloud with a T_T of -17 °C, yet on another day with a T_B of -8 °C and the same T_T there might be only 1 L^{-1} of ice particles in an aging cloud. However, for both days a significant correlation will exist between I_M and T_T. This illustrates how two researchers sampling continental cumuliform clouds in the same region, but on days with different cloud-base temperatures, could reach quite different conclusions concerning the presence of high ice particle concentrations at a particular cloud-top temperature.

Our measurements reveal a dependence of I_M on T_T for continental cumuliform clouds, but it is one-half to two orders of magnitude *less* than the temperature dependence of conventional ice-nucleus measurements (i.e. Fletcher's relation). This was deduced by comparing I_M in clouds with similar values of D_T but different T_T values for clouds with $T_T \leqslant -10$ °C. For the clouds with a broad droplet spectrum ($D_T \geqslant 24$ μm diameter):

$$I_M = 0.4 \exp(-0.23\, T_T). \tag{8}$$

Hence, in this case I_M increases by about a factor of 10 as T_T falls from -15 to -25 °C (conventional ice-nucleus measurements indicate that I_M should increase by about two orders of magnitude for this decrease in temperature). For the clouds with a narrow droplet spectrum:

$$I_M = 1.9 \times 10^{-3} \exp(-0.38\, T_T). \tag{9}$$

In this case, I_M averages about 0.5 L^{-1} for $T_T = -15$ °C, but is 3–7 L^{-1} for $T_T = -22$ °C. Thus, I_M increases by about one order of magnitude for a decrease in temperature of 7 degC; conventional ice-nucleus measurements show an increase in I_M of nearly two orders of magnitude for a 7 degC decrease in temperature. It should be noted that all of these clouds still contained liquid water at or near cloud top before the formation of the maximum ice particle concentration. We suspect that when the liquid water is depleted, I_M does not increase with decreasing temperature (see Hobbs and Rangno 1990a).

(*f*) *Maximum ice particle concentrations and the breadth of the droplet spectrum*

Hobbs and Rangno (1985) showed a strong correlation between the maximum ice particle concentrations (I_M) that developed in cumuliform clouds and the breadth of the droplet size distribution near cloud top (as measured by D_T). The relationship between D_T and I_M for the new data reported here on mature and aging continental cumuliform clouds with widths $\geqslant$2 km (similar to the cloud widths sampled by Hobbs and Rangno (1985)) is shown in Fig. 8. In spite of the wide range of T_T values (from -6 °C to -32 °C), D_T is still a better predictor of I_M ($r = 0.71$) than is T_T ($r = 0.61$). Further, for the subset of data comprising most of our clouds (i.e. those with $T_T \geqslant -25$ °C) the correlation between I_M and D_T rises to 0.78, while that between T_T and I_M is 0.58. Other surrogates for liquid-water content, such as cloud depth or the concentration of droplets with diameter >24 μm, also correlate significantly with I_M.

The empirical relationship between I_M (L^{-1}) and D_T (μm) for the new data set (circles and solid line in Fig. 8) is:

$$I_M = \left(\frac{D_T}{21}\right)^{10.6}. \tag{10}$$

The maximum ice particle concentrations found by Hobbs and Rangno (1985) in cumuliform clouds are generally higher than those found in the present study even though cloud-top temperatures are similar. This is because, in general, wider clouds, which tend to have higher maximum ice particle concentrations, were sampled by Hobbs and Rangno (also discussed by Rangno and Hobbs (1991)). For the Hobbs and Rangno 2-D cloud probe data set, as reprocessed by Rangno and Hobbs (triangles and dashed line in Fig. 8), the corresponding relationship is:

$$I_M = \left(\frac{D_T}{17}\right)^{8.3}. \tag{11}$$

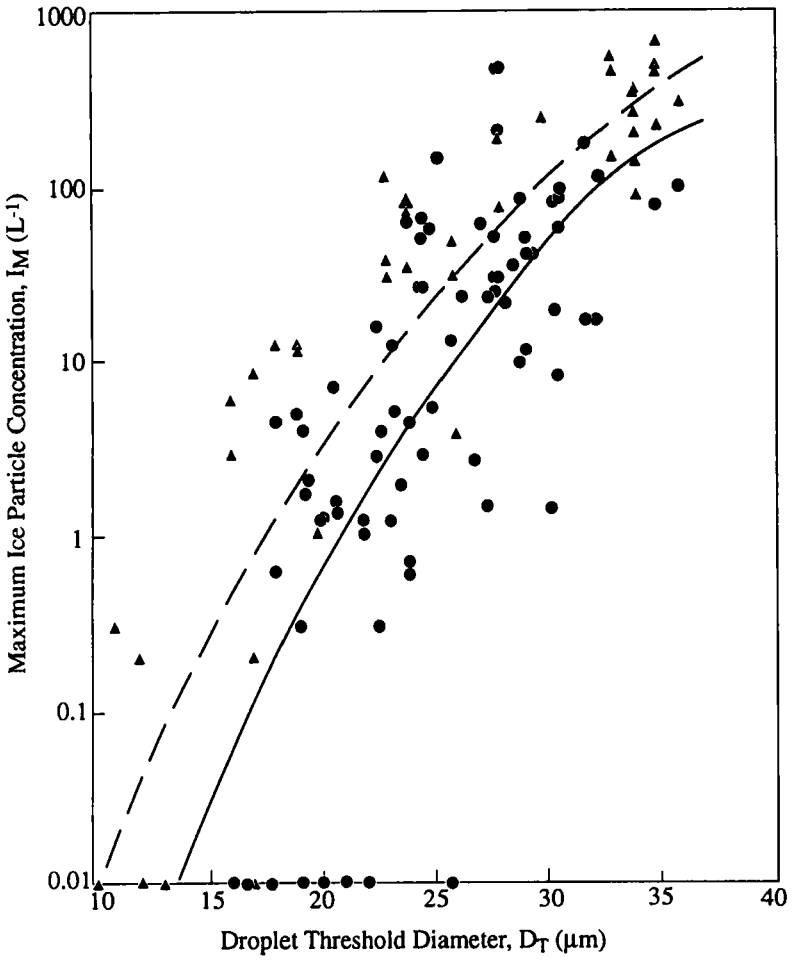

Figure 8. Maximum ice particle concentrations (I_M) versus droplet threshold diameter (D_T) for the new data set on mature and aging continental cumuliform clouds with top temperatures ≤6 °C (circles) and widths ≥2 km. The triangles are data points from Hobbs and Rangno (1985) for mature and aging continental cumuliform clouds. The dashed line is the I_M versus D_T relation from Hobbs and Rangno (1985)—Eq. (11) in the present text; the solid line is the corresponding relation for the new data set—Eq. (10) in the present text.

4. Some illustrative case studies

We will now illustrate some of the interesting ice-forming characteristics of small continental cumuliform clouds, which have been described in general in the preceding section, by decribing several case studies.

(*a*) *Cold cloud tops, a narrow droplet spectrum, and low ice particle concentrations*

The clouds sampled on 3 February 1989 exemplify the dampening effect of a quite narrow droplet size spectrum ($D_T \leqslant 20\ \mu m$) on the production of ice particles even when the cloud-top temperature is quite low (−26 °C).

The flight took place over the Canadian coastal waters near Vancouver Island, following a surge of extremely cold, arctic air into western Canada and the Pacific Northwest. A strong upper-air vortex with a central temperature of −45 °C at 500 hPa lay along the Washington coast. The wind was easterly at the surface through 700 hPa. The temperature at 850 hPa was −18 °C. The dry offshore flow of continental air was moistened rapidly by the strong low-level instability over the coastal waters. This led to the formation of cumulus fractus and cumulus humilis clouds about 50 km from the coastline, and cumulus mediocris and stratocumulus cloud complexes, tens of kilometres wide and about 0.9 km in maximum depth, at about 100 km offshore. The tops of the clouds were confined by a strong temperature inversion. Cloud bases were located near 860 hPa, or about 1.5 km above sea level, and they descended slightly and increased in temperature toward the west (from −18 °C near where the clouds first appeared to −16.5 °C about 100 km offshore). Cloud-top temperatures ranged from −20 to −26 °C, and their height increased downwind. Maximum liquid-water content in these clouds was $\leqslant 0.4\ g\ m^{-3}$ near cloud top. Virga, many kilometers in extent, were observed from the bases of the wider cloud complexes; generally ice was not detected in small cumuliform clouds at the upwind edge of the cloud region nearest the coastline. None of the precipitation encountered reached the ground. Extensive areas of whitecaps were visible on the ocean surface, and moderate to heavy turbulence was observed from cloud top to within 50 m of the ocean surface. The droplet spectra in these clouds were narrow, with $D_T = 16$–$20\ \mu m$ in the upper regions of the cumulus and stratocumulus clouds where the highest liquid-water contents were encountered. Droplet concentrations averaged about $350\ cm^{-3}$. (In this region, *maritime* clouds have average droplet concentrations of about $80\ cm^{-3}$ and $D_T > 30\ \mu m$.)

In spite of the relatively low cloud-top temperature, the maximum concentration of ice particles encountered on this day was only $7\ L^{-1}$. This is the lowest maximum concentration of ice particles that we have measured in aging cumuliform clouds with such a low cloud-top temperature. However, the maximum ice particle concentrations measured on this day are similar, although lower than those expected from conventional ice-nucleus measurements. Figure 9 shows a five-minute segment of cloud microstructure, 35 GHz radar data, and 2-D PMS particle imagery that typified the data collected on this flight. The ice particles collected on glass slides were thick plates and short columns, which clumped into a few aggregates near and below cloud base.

(*b*) *Cold cloud tops, a broad droplet spectrum, and high ice particle concentrations*

The measurements on 16 October 1990 illustrate the effect on ice particle concentrations of a broad droplet size spectrum near cloud top. Even though the lowest cloud-top temperature was 1.5 degC higher than the case described above, many more ice particles were present.

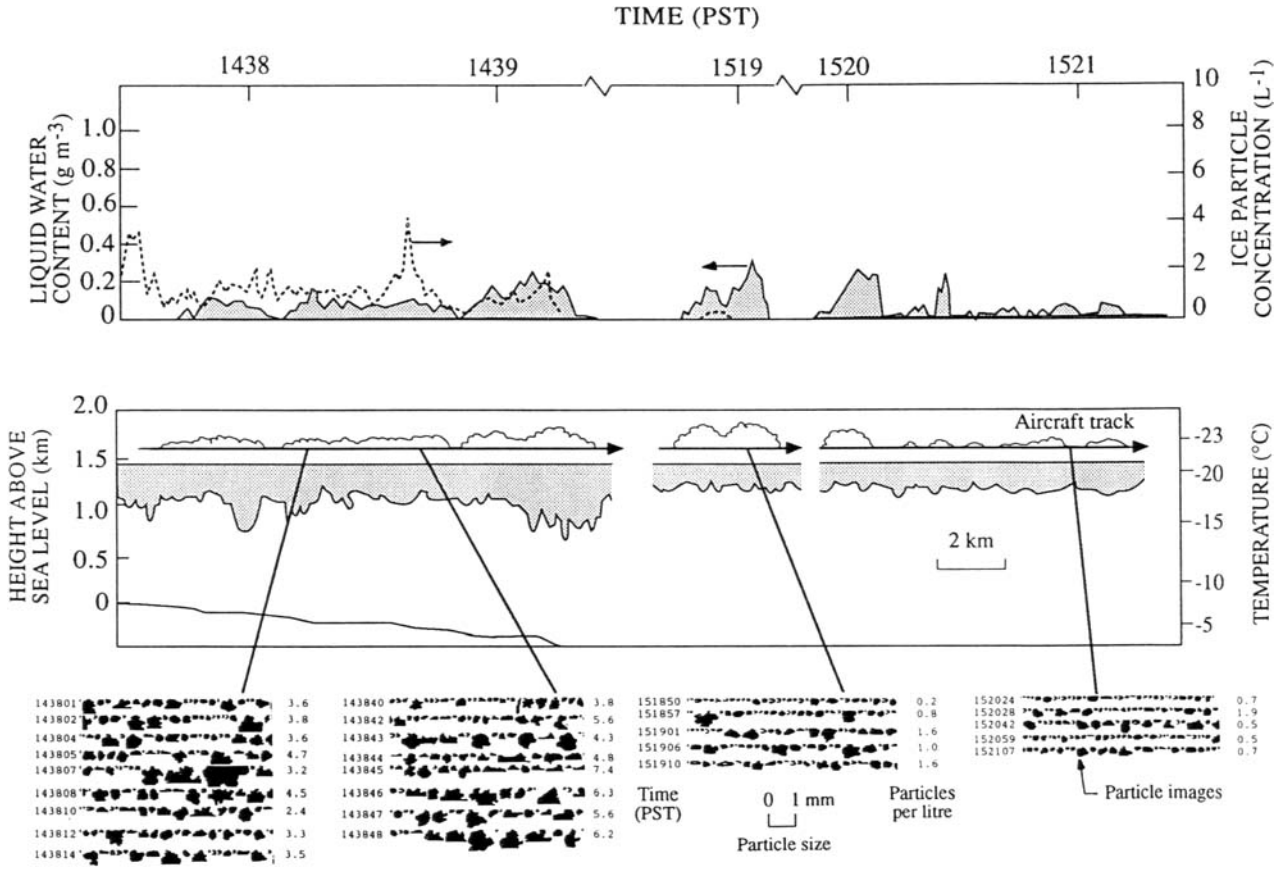

Figure 9. Some microstructural measurements in continental cumulus humilis and stratocumulus clouds on 3 February 1989. The top panel shows liquid-water content (shaded) and ice particle concentrations (broken line). The middle panel indicates radar echo returns from a downward-pointing 35 GHz radar aboard the aircraft, light shading indicates a minimum detectable radar echo and the scalloping shows the approximate upper boundary of the cloud; also indicated is the aircraft flight track. Shown on the right are air temperatures at the heights shown on the left. The lower panel shows samples of the PMS 2-D cloud-probe imagery and particle concentrations along the flight track at the locations and times indicated.

On this day, as an upper-level trough exited Washington State under a north-westerly flow, a few late afternoon cumulus and small cumulonimbus clouds developed over the plains of eastern Washington. Cloud bases were at 730 hPa with temperatures of −6.5 °C. Droplet concentrations in the young portions of the clouds were ~650 cm^{-3}. Maximum liquid-water contents in the upper regions of the young clouds were about 0.8 g m^{-3} and $D_T = 26\ \mu m$. The lowest cloud-top temperature was −24.5 °C.

A multi-turreted, but isolated, cumulonimbus cloud, about 10 km wide and 2.3 km deep, which was producing a broad shaft of snow, was chosen for study. An upshear turret had visibly converted to ice on the western side of the cloud several minutes before the aircraft reached cloud base, but no new turrets followed. Thus this cloud was already in a maturing-to-dissipating stage as the aircraft began to climb from cloud base. A light (transparent) rain shower reached the ground below the level where the snow melted.

The maximum ice particle concentration measured in this cloud was 60 L^{-1}, with wide regions within the cloud with ice particle concentrations of 20–50 L^{-1}. The ice particles included many aggregates but no attempt was made to estimate the number of single crystals in the aggregates. No graupel, and only traces of liquid water, were encountered. A typical segment of the microstructural measurements, 35 GHz data and 2-D PMS particle imagery, obtained in this cloud is shown in Fig. 10.

(*c*) *Moderately cold cloud tops, a narrow droplet spectrum, and low ice particle concentrations*

May 11 1989 is illustative of the microstructure of relatively simple cumulus mediocris continental clouds, only about 1 km deep. Cloud tops were moderately supercooled (T_T about −15 °C). The base of the clouds was at 715 hPa with a temperature of −8 °C. Not surprisingly, few ice particles formed.

The clouds formed in a north-westerly flow topped by a strong stable layer that restricted cloud growth. The clouds formed both separately and in clusters several kilometres long in the downwind direction. Transparent regions of virga or ice particles were observed, sometimes below cloud bases but often at and beyond the downwind edges of the clouds as 'ghosts' of previous droplet clouds from which they originated. No precipitation reached the ground.

Droplet concentrations in the youngest portions of the clouds were ~350 cm^{-3}. The droplet spectrum near cloud top was narrow ($D_T = 19\ \mu m$). The maximum ice particle concentration that was measured was only about 1 L^{-1}, and most of the clouds had ice particle concentrations of 0.2 to 0.4 L^{-1}. The 2-D PMS imagery showed the ice particles to be regular stellar/dendritic crystals, nearly all intact and with no aggregation. The ice particle size spectrum was broad, indicating a slow, steady production of new ice particles. The concentrations of ice particles were near or slightly above those expected from conventional ice-nucleus measurements.

Figure 11 shows a sample of the microstructural measurements, 35 GHz radar data, and 2-D PMS particle imagery collected in these clouds.

(*d*) *Moderately cold cloud tops, a broad droplet spectrum, and high ice particle concentrations*

The measurements obtained on 10 August 1990 typify the effect of a broad droplet spectrum in producing high ice particle concentrations even when cloud-top temperatures are not very low.

On this day cumuliform clouds formed over eastern Washington State in air that had originated in low latitudes and had flowed northward over Washington State around

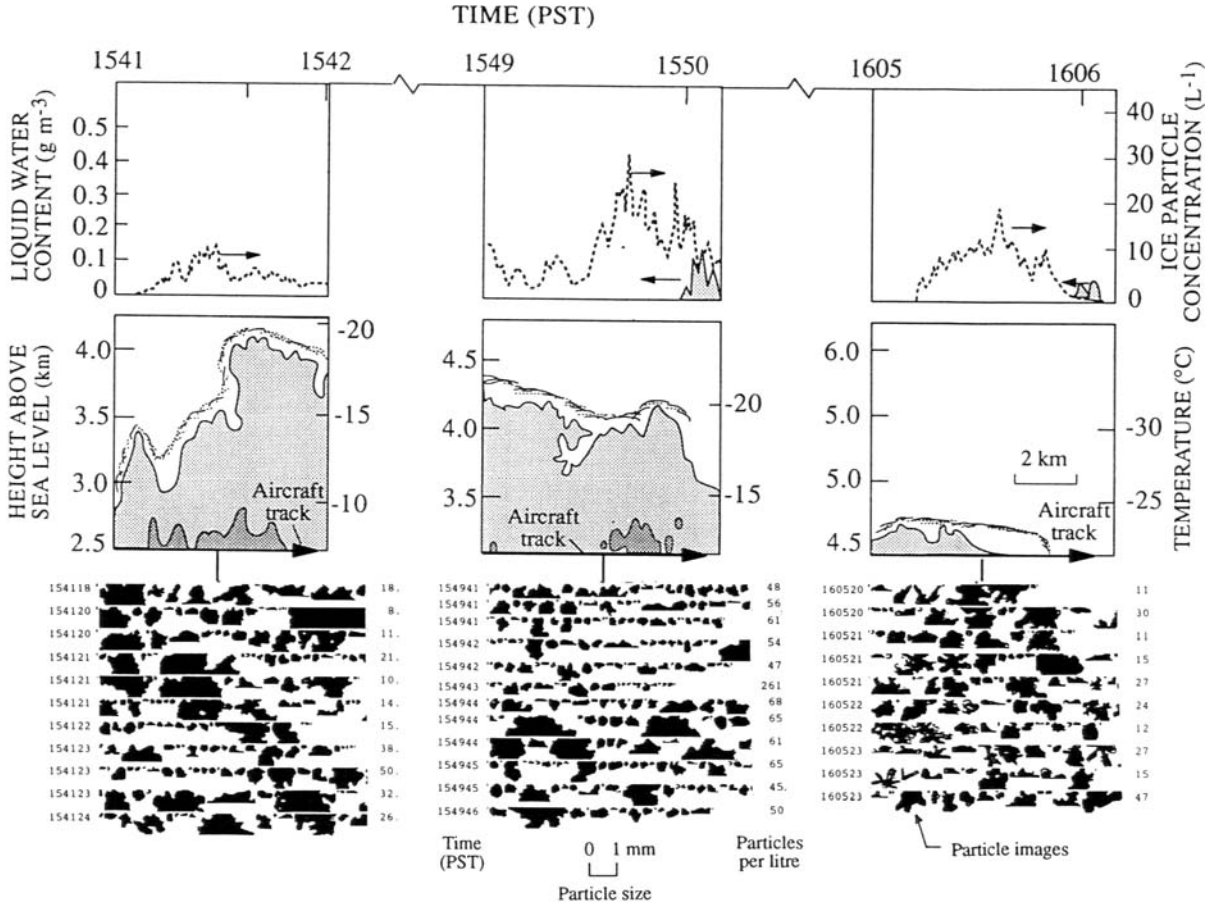

Figure 10. As for Fig. 9 but for 16 October 1990 in a small continental cumulonimbus capillatus cloud. The light shading indicates the minimum detectable radar echo and the darker shading the next higher radar echo intensity. (In this case the airborne radar was pointed upward.)

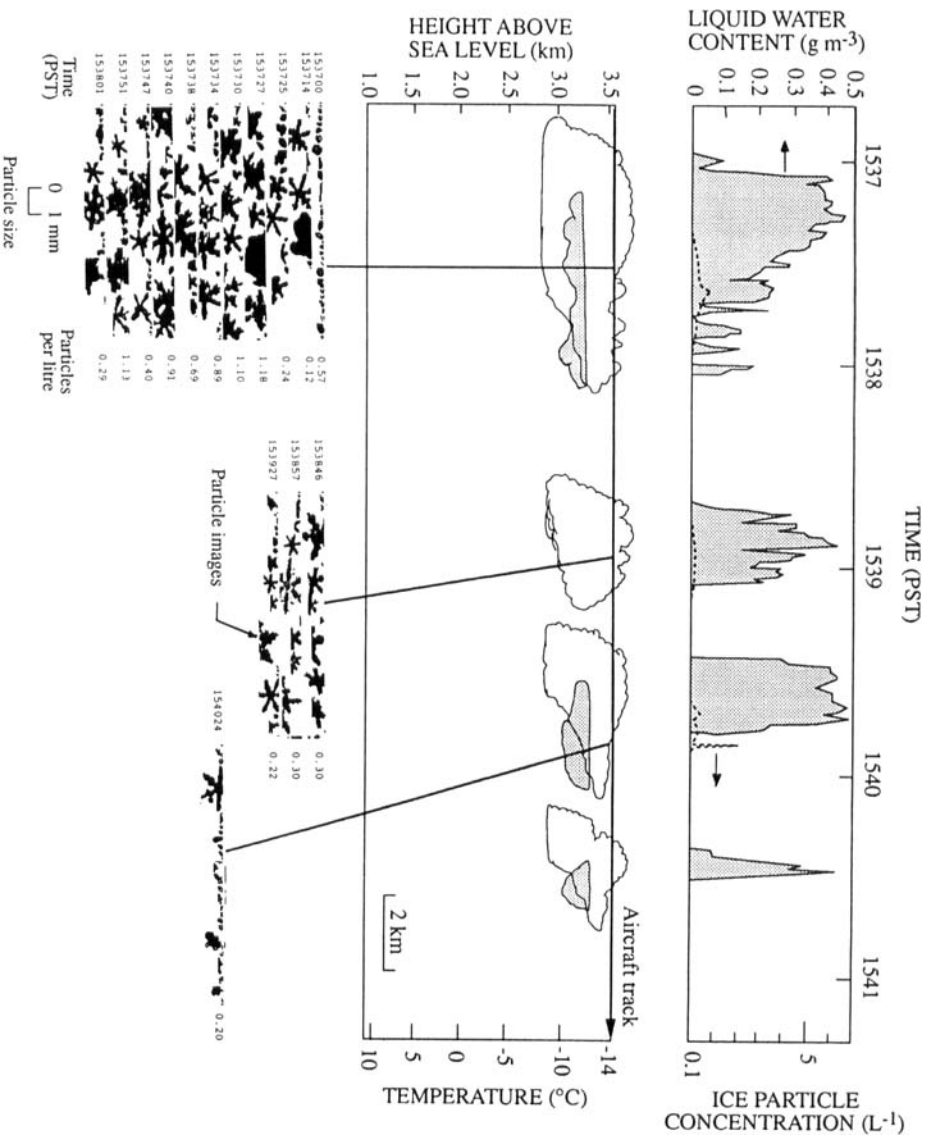

Figure 11. As for Fig. 9 but for 11 May 1989 in continental cumulus mediocris clouds.

the western periphery of a strong upper-level anticyclone. Cloud bases were at 640 hPa with temperatures of 0 °C. The lowest temperatures of the clouds studied on this day were about −20 °C. Droplet concentrations in the youngest cloud portions just above cloud base were ~500 cm^{-3}. Because of the relatively cool cloud base, and high droplet concentrations, droplets >23 μm diameter were marginally present in the riming–splintering temperature zone (see, for example, Mossop 1985a). The maximum droplet concentrations measured in the wettest regions (defined as those with liquid-water content $\geq 0.3\ g\ m^{-3}$) of this zone were $\leq 7\ cm^{-3}$. Further, these concentrations were confined to temperatures ≤ −6.5 °C, where riming and splintering is much less efficient than at −5 °C (e.g. Mossop 1978, 1985b). At −5 °C the concentrations of droplets ≥23 μm in diameter averaged 1–2 cm^{-3}. However, the droplet spectrum was quite broad in younger clouds that reached above this temperature level. For example, D_T = 28–29 μm in young cumuliform clouds at flight levels of 2.2 km above cloud base where the temperature was −13 °C and colder.

Five aircraft passes were made through a modest cumulonimbus complex a few kilometres wide between 1635 and 1711 PST (Pacific Standard Time equals GMT minus 8 hours). This cloud consisted of multiple turrets with a lowest T_T of −15 °C. The passes were made at increasingly higher levels in steps of about 300–400 m, beginning with a pass at 574 hPa and −5.5 °C. Millimeter-sized graupel was encountered intermittently in all the passes. The maximum ice particle concentration on the first pass was ~3 L^{-1}, mostly comprised of graupel, some of which had already reached more than 1 mm in diameter. The ice particle maxima in the following passes were 2, 80, 170, and 110 L^{-1}, respectively. These passes began, respectively, at 5, 18, 26, and 36 min after the first pass. The upward-pointing 35 GHz radar indicated that at least some of the precipitation that reached the aircraft during all of the passes had descended from near cloud top, and that the highest cloud tops in this complex of turrets were relatively constant in height during the period of study. Columnar ice particles, sometimes in high concentrations (tens per litre), were detected in limited cloud regions between −4 and −10 °C. However, columnar ice particles constituted only about 10% of the total 2-D PMS cloud-probe images during the five passes through this cloud. The highest concentration of millimeter-sized graupel, averaged from the beginning to the end of each graupel occurrence, was 0.34 L^{-1}, which was measured in the fourth aircraft pass after high ice particle concentrations had developed. Graupel concentrations increased from 0.05 to 0.09, and then to 0.25 L^{-1}, in the three previous passes. The greatest graupel concentration, averaged over 1 s of flight time (or 94 m), was 3.7 L^{-1}; this was also measured in the fourth pass. Regions of rather uniformly sized ice particles in high concentrations were encountered during the third, fourth, and fifth passes.

During the third pass, at −9 °C, the graupel were accompanied by relatively uniformly sized ice particles, most of which were <500 μm diameter, in concentrations ranging from ~40 to 100 L^{-1} over 2 km of path within the cloud. The size of these particles indicates that they had formed within the previous 10 min. A further indication that these ice particles had formed rather suddenly was the simultaneous presence of liquid water. These particles were stubby columnar and quasi-spherical in shape. Similar relatively uniformly sized ice particles in higher concentrations, but containing very few columnar crystals, were encountered in the fourth and fifth passes.

A sample of the microstructural measurements, 35 GHZ radar imagery, and 2-D PMS particle imagery made in this cumulonimbus complex is shown in Fig. 12. Typical ice crystal replicas showed the predominance of non-columnar crystals in these clouds.

The rate of splinter production due to the riming–splintering mechanism is given approximately by (e.g. Willis and Hallett 1991):

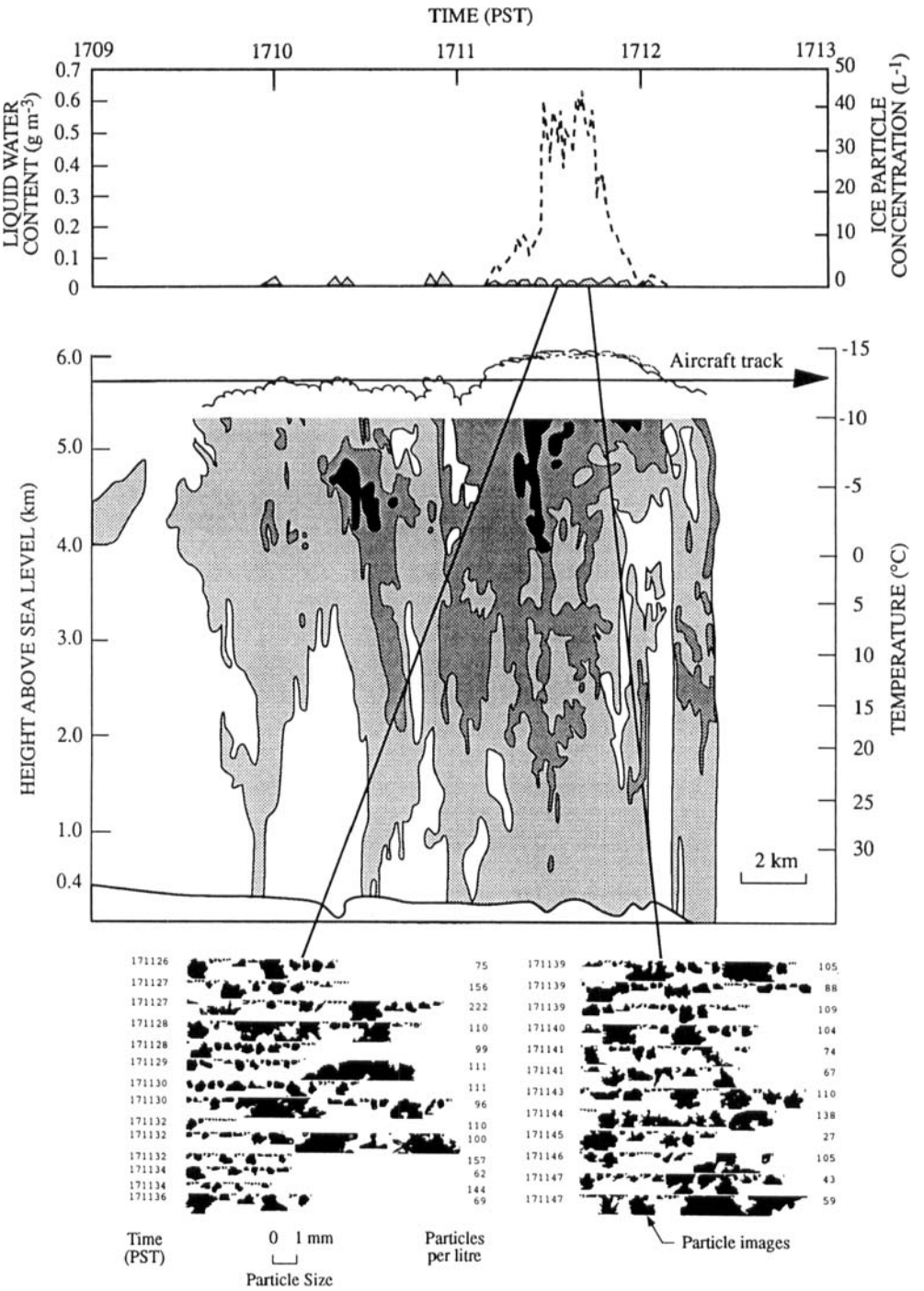

Figure 12. As for Fig. 9 but for 10 August 1990 in a small continental cumulonimbus capillatus cloud. The light shading indicates the minimum detectable radar echo, the darker shading the next higher radar echo intensity, and the darkest shading the highest radar echo intensity.

$$\frac{(N_g N_d V_g D E)}{800} \tag{12}$$

where, N_g is the concentration per litre of graupel of diameter D (mm) falling with velocity V_g (m s^{-1}), N_d the concentration (cm^{-3}) of droplets $\geqslant 24$ μm diameter collected with efficiency E, and it is assumed that 200 collected droplets produce one ice splinter. For the case considered here we take: $N_d = 3$ cm^{-3} at -5 °C, $N_g = 0.5$ L^{-1}, $V_g = 1.5$ m s^{-1}, $D = 1.25$ mm, and $E = 0.75$. These values, which are somewhat generous for the production of ice splinters, lead to a production rate of about 0.01 splinters per litre per second, or an ice particle concentration due to riming–splintering of ~6 L^{-1} over a 10 min period. Thus it would appear that riming–splintering alone cannot account for the high concentrations of small ice particles (~100 L^{-1}) that formed within ~10 mins and were intercepted in large regions of this cloud. Also, the highest concentrations of graupel were measured *after* the highest ice particle concentrations were measured, not before as would be expected from a riming–splintering mechanism.

(*e*) *Very cold cloud bases and tops, a broad droplet spectrum, and high ice particle concentrations*

The data collected on 18 May 1989 typify the formation of ice particles at very low temperatures and in the presence of a broad droplet spectrum.

On this day a strong, upper-level trough was crossing Washington State; 500 hPa temperatures were below -30 °C. Cloud base temperature was -10.5 °C at 710 hPa and the coldest cloud tops were -32.5 °C at about 500 hPa. The depth of the deepest clouds was 2.7 km. Liquid-water contents of up to 0.8 g m^{-3} and ice particle concentrations <3 L^{-1} were measured in young turrets at -26 °C. The breadth of the droplet spectrum near these cloud tops, as measured by the threshold diameter D_T, was 28 μm. Heavy, clear icing was observed on the aircraft, also indicative of larger cloud droplets. The maximum ice particle concentration measured on this day was 450 L^{-1}, in the dissipating region of one of the coldest clouds.

Ice particles formed in upward moving air, just before cloud collapse. In the building cumulus clouds at -20 °C a few ($<5\%$) of the total ice particle concentration were stellar and dendritic ice crystals or their fragments. These particles must have originated from below the level at which they were collected. This was the only flight in the current series in which evidence was obtained for ice particles being carried upward over a significant distance. The formation of ice particles in the updraught on this day was probably due, in part at least, to the very low temperatures.

A striking aspect of the PMS 2-D particle imagery, and one that was observed on some other flights with a broad droplet spectra near cloud top, was the rapidity with which high concentrations of ice particles appeared in the maturing-to-dissipating stage of the life cycle of the cloud. The speed at which these high concentrations of ice particles appeared was deduced from their relatively uniform and small sizes. Figure 13 (lower) shows the ice particles imaged during a pass through one of the regions of high ice particle concentration on 18 May 1989. Since nearly all of these ice particles are <500 μm diameter, they must have formed in <10 min. In spite of ice particle concentrations >200 L^{-1}, liquid water was occasionally present in amounts up to 0.4 g m^{-3}. This is further evidence of the suddenness with which the ice particles must have formed. Graupel >1 mm in diameter was often present with the high concentrations of small ice particles, and a few ice aggregates were present. Replicas of hexagonal plates were collected at temperatures below -25 °C. Figure 13 shows a sample of microstructural

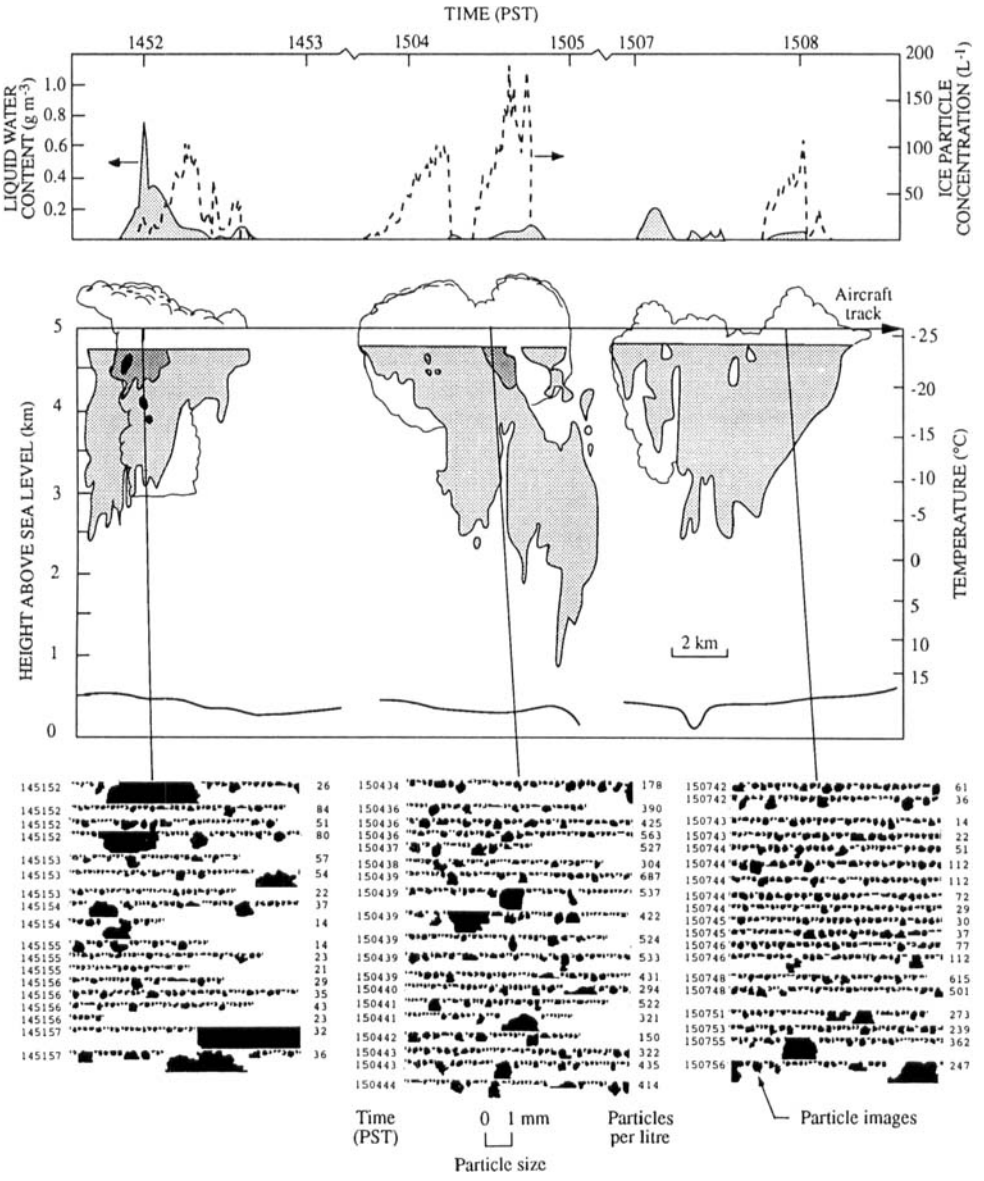

Figure 13. As for Fig. 9 but for 18 May 1989 in a small, but very cold, continental cumulonimbus capillatus cloud. The shadings are as described in Fig. 12.

measurements, 35 GHz radar echoes, and 2-D PMS particle imagery acquired during the sampling of these clouds in one of the regions of maximum ice particle concentrations.

(*f*) *High cloud-base temperature, moderately cold cloud tops, a broad droplet spectrum near cloud top, and high ice particle concentrations*

August 20 1990 had the highest cloud-base temperatures and the highest D_T (31 μm) encountered in the present study. It illustrates that the highest ice particle concentrations measured (75 L^{-1}), consisting primarily of ice columns, were probably due to riming–splintering. However, relatively high concentrations of ice particles (tens per litre),

comprised of non-columnar, quasi-spherical, particles were also encountered in the upper portions of the cloud above the riming–splintering zone. This suggests that another ice-forming mechanism, along with riming–splintering, contributed to the ice particle concentrations in the cloud.

On this day an easterly flow around an upper-level cyclone situated to the south of Washington State brought moist tropical air into eastern Washingston State. Cloud-base temperature was 8 °C at 760 hPa. Drizzle drops ($\geqslant 100\ \mu$m diameter) in concentrations $<0.01\ L^{-1}$ were observed in the upper regions of cumulus congestus clouds that were about 2 km thick or reached the −5.5 °C level. This was our only observation of drizzle drops in the continental clouds of eastern Washington State. Droplet concentrations in rising cloud regions were about $400\ cm^{-3}$. The maximum liquid-water content measured was $1.4\ g\ m^{-3}$ at −8 °C. (Undoubtedly, higher liquid-water contents were present in the cumulonimbus cloud described below during its rise to −15 °C.)

An isolated, dissipating cumulonimbus cloud, with a cloud-top temperature of −15 °C, was chosen for study. From its ragged, frayed appearance, weak-looking, narrow upshear cumuliform turrets, the low concentration of liquid water when the cloud was first sampled, and the presence of numerous ice aggregates, we deduced that this cloud was sampled after the ice particles had reached their maximum concentrations. Above this cumulonimbus cloud was a layer of altostratus opacus. The maximum concentrations of droplets >23 μm diameter measured in nearby young clouds at the bottom and top of the riming–splintering temperature zone were 25 and $40\ cm^{-3}$, respectively. The maximum observed ice particle concentration, in any of the several passes through this cloud, was $75\ L^{-1}$ at −7 °C. Columnar crystals constituted about half of these ice particles. The maximum measured liquid-water content was $0.6\ g\ m^{-3}$, encountered in a younger but weak upshear turret adjacent to the region of highest ice particle concentrations. The maximum average and peak 1 s concentrations of graupel, 0.7 and $4.6\ L^{-1}$, respectively, were also measured on this pass. The smaller quasi-spherical particles in the 2-D PMS imagery were probably plate-like crystals; hexagonal plates were replicated on slides exposed in this cloud.

Figure 14 shows an example of the microstructural features of this cloud obtained on one of the several passes along an upshear/downshear line. The rise in ice particle concentrations seen about midway through this pass was due to higher concentrations associated with columnar ice particles, which we attribute to riming–splintering.

If we assume for this case that $N_d = 25\ cm^{-3}$ at −5 °C, $N_g = 1.0\ L^{-1}$, $V_g = 1.5\ m\ s^{-1}$, $D = 1.25$ mm, and $E = 0.75$, substituting these values into (12) leads to a production rate of about 0.14 ice splinters per litre per second, or about $80\ L^{-1}$ of ice particles over a 10 min period. Thus, it would appear that riming–splintering might account for the high concentrations of small ice particles that were measured in this cloud, presuming that graupel was present in concentrations as high as $1\ L^{-1}$ before the development of the small ice particles. However, it should be noted that the highest concentrations of graupel were, in fact, measured *after* the cloud had formed copious small ice particles.

5. Summary and discussion

In previous studies (Hobbs and Rangno 1990a; Rangno and Hobbs 1991; Hobbs and Rangno 1985) we documented some of the microphysical factors that affect the development of ice and precipitation in maritime cumuliform clouds. The present paper has extended this study to continental cumuliform clouds. Our principal results for cumuliform clouds *in general* can now be summarized as follows:

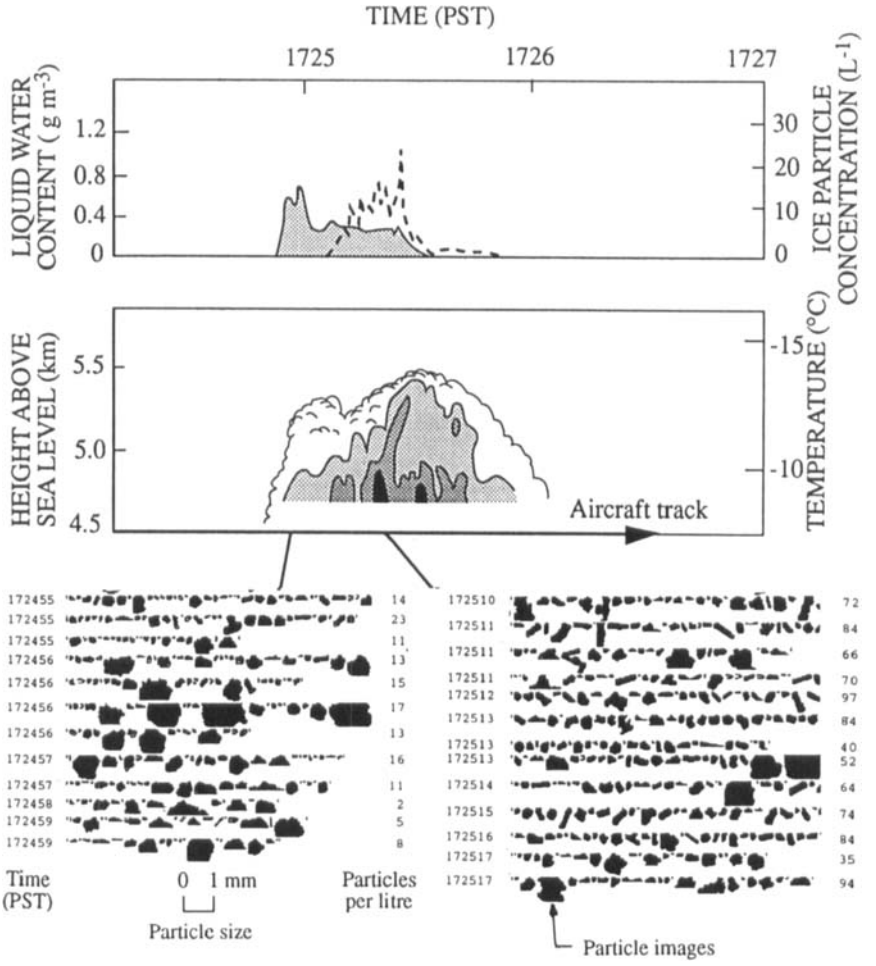

Figure 14. As for Fig. 9 but for 20 August 1990 in a small continental cumulonimbus capillatus cloud. The shadings are as described in Fig. 12. (In this case the airborne radar was pointed upward.)

(i) The initiation of ice and the maximum concentrations of ice particles that form in wider (>2 km) maritime and continental cumuliform clouds are related to the largest droplet sizes near cloud top before the formation of appreciable ice. Our earlier measurements in maritime cumuliform clouds (e.g. Hobbs and Rangno 1985) indicated that D_T near cloud top had to exceed about 20 μm diameter, and T_T had to be ≤ -6 °C, for the initiation of ice. Our more recent measurements in continental cumuliform clouds show that the required value of T_T for ice initiation depends on D_T near cloud top. For example, it can be seen from Fig. 1(*c*) that D_T must be about 25 μm diameter for the onset of ice at T_T near -13 °C, but D_T must be about 35 μm diameter for the initiation of ice at T_T near -5 °C.

(ii) The higher the cloud-base temperature, the higher the temperature at which ice first appears at or near cloud top. This finding supports an observation of Ludlam (1952). This is due to the dependence of ice initiation on the size of the largest drops near cloud top. Generally, the higher the cloud-base temperature the larger are the droplets at any given level in a cloud.

(iii) Once ice appears the increase in ice particle concentration with decreasing T_T is more rapid the broader the initial droplet size distribution near cloud top. Thus a family of curves exists that relate I_M to T_T (Fig. 7) and, therefore, to cloud depth.

(iv) If a cumuliform cloud has a relatively broad droplet size distribution near cloud top ($D_T > 24\ \mu m$), high ice particle concentrations (tens to hundreds per litre) can appear very suddenly (≤ 10 min). This suggests a two-stage ice-forming process (Hobbs and Rangno 1990a; Rangno and Hobbs 1991). In the first stage ice particle concentrations are low (usually a few per litre or less). In the second stage high concentrations of pristine ice crystals appear very rapidly near cloud top. However, the second stage is most apparent when sufficient concentrations of large droplets are present near cloud top, and the top resides at or very near the maximum cloud-top height for more than a few minutes.

(v) Ice particle concentrations increase by a factor of about ten for every 7 degC drop in temperature for clouds with a narrow droplet size distribution ($D_T < 20\ \mu m$ diameter) near cloud top. For clouds with a broad droplet size distribution near cloud top ($D_T > 24\ \mu m$), which exhibit the second stage of ice formation, maximum ice particle concentrations increase by a factor of only about ten for every 10 degC decrease in cloud temperature once the second stage is underway. Indeed, once the liquid water has been depleted, no further ice particles form even if the top continues to cool (e.g. Hobbs and Rangno 1990a).

(vi) Narrow (≤ 2 km wide in their upper portions), short-lived, 'chimney' clouds with subsiding tops do not produce as many ice particles as wider clouds (cf. Fig. 5). This observation supports the findings of Mossop *et al.* (1970, 1972). These chimney clouds appear to exhibit only the first stage of ice particle formation, even when $D_T > 24\ \mu m$ near cloud top. Since Schemenauer and Isaac (1984) and Isaac (1986) found that the width of a cloud near its top is a good measure of the duration of cloud-top lifetime at a particular level, the low ice particle concentrations found in narrow chimney clouds could be due to the short time spent by the cloud tops at their minimum top temperature. However, the high concentrations of small, and relatively uniform-sized, ice particles encountered in wider cumuliform clouds indicate that the cloud-top lifetime required for prolific ice formation is only a few minutes longer than that for a chimney cloud. The maximum ice particle concentrations in *chimney clouds* are similar to recent ice-nucleus concentrations summarized by Meyers *et al.* (1992).

(vii) Our observations of a two-stage ice-forming process in cumuliform clouds that have an especially broad droplet spectrum near cloud top is compatible with radar observations of sudden echo formations in vigorous cumulonimbus cloud that extend rapidly upward and downward (e.g. Battan 1953; Knight *et al.* 1983; Raymond and Blyth 1989). We attribute this to high concentrations of small ice particles being carried upward while the largest graupel particles descend. The multiple Doppler-radar observations of precipitation development in continental cumuliform clouds in New Mexico by Raymond and Blyth (1989) are especially pertinent from this point of view. They concluded that nearly all of the precipitation particles in a convective cell originated during an explosive stage that started soon after the initial radar echo formed just above the -10 °C level. This 'big bang' precipitation-forming event is similar to the type of rapid ice formation that we and others have discussed (Koenig 1963; Sax *et al.* 1976; Hobbs and Rangno 1990a; Rangno and Hobbs 1991; Gayet and Soulage 1992).

Our findings support observations indicating that cloud depth is a more important determinant of ice particle development than is cloud-top temperature (Morris and

Braham 1968; Hobbs and Rangno 1985, 1987). Earlier workers (e.g. Battan 1963) considered the relationship between cloud depth and the onset of precipitation as support for the collision–coalescence process of precipitation formation. Our studies indicate that this relationship could also be due to the dependence of the first stage of ice formation on the size of the largest droplets and, therefore, on cloud depth.

Our findings suggest that the *initial* ice particles that form in continental and maritime cumuliform clouds originate through the freezing of droplets, particularly larger droplets, and that the freezing temperatures of these droplets increase as their sizes increase (e.g. Fig. 1(c)). Contact nucleation is a candidate for the freezing of the droplets, since many laboratory experiments have also shown that this mode of nucleation causes freezing at relatively high temperatures and is dependent on drop size (e.g. Blanchard 1957; Gokhale and Spengler 1972; Pitter and Pruppacher 1973; Vali 1971). However, while contact nucleation may initiate ice in clouds at relatively high temperatures, it seems unlikely that it can account for the high concentrations of small ice particles that we have observed in the second stage of ice formation (Baker 1991; Beard 1992).

Rosinski (1991) suggested that droplet freezing in clouds could be due to high temperature ice-forming nuclei (HTIFN) that derive from cloud condensation nuclei from the ocean. His measurements suggested that HTIFN may be present in concentrations of $0.2\,L^{-1}$ at temperatures between -9 and $-12\,°C$ provided that the supersaturation with respect to water is ~10%. The concentrations of HTIFN found by Rosinski supports some of the observations and speculations of Hobbs and Rangno (1985, 1990a) and Rangno and Hobbs (1991). For example, we have observed ice particles in concentrations between 0.1 and $1\,L^{-1}$ at the beginning of the ice-forming process in clouds with tops with temperatures between -9 and $-12\,°C$. Rosinski found that the temperature at which particles collected over the ocean became active as ice nuclei increased following a condensation–evaporation cycle. Ice nuclei subjected to such a cycle were measured in concentrations of $0.7\,L^{-1}$ at $-10\,°C$ and $7\,L^{-1}$ at $-17\,°C$, which are close to the concentrations of ice particles in what we have called the first stage of ice formation. These concentrations are higher (by more than an order of magnitude) than conventional ice-nucleus concentrations (e.g. Fletcher 1962). However, they are similar to more recent ice-nucleus concentrations measured with filters, and in continuous-flow diffusion chambers (Meyers *et al.* 1992).

On the other hand, the fact that continental *and* maritime clouds exhibit a first stage of ice formation suggests a common formation mechanism, which is unlikely if the responsible ice nuclei derive from the ocean. For example, our flight of 3 February 1989, discussed in section 4(a), indicates that the ocean did not provide a source of HTIFN. On this day, clouds with $D_T < 20\,\mu m$ and $T_T = -26\,°C$ formed over the ocean in an offshore flow. The widespread (>30 km wide in some areas) and largely liquid stratocumulus and cumulus clouds were likely to have contained many particles that had been processed previously by clouds (i.e. subjected to a condensation–evaporation cycle). The boundary layer was well mixed, with turbulent flying conditions to within 50 m of the ocean surface, where a superadiabatic lapse rate was present. In other words conditions were conducive for the transport of HTIFN from the ocean into the clouds. Yet maximum ice particle concentrations in these clouds were only $3–7\,L^{-1}$. These are the lowest concentrations that we have measured in clouds with top temperatures this low. These concentrations are, however, similar to those for ice-nucleus concentrations given by Meyers *et al.* (1992).

The maximum concentrations of ice particles that develop during the second stage of ice formation are often far higher than even those suggested by Rosinski or Meyers *et al.* For example, in our case study of 10 August 1990 $I_M = 170\,L^{-1}$, with $T_T = -15\,°C$.

These high ice particle concentrations appear to be due only partially to the riming–splintering mechanism (Hallett and Mossop 1974; Mossop 1985b), because columnar crystals were rare and conditions for the operation of the riming–splintering mechanism were marginal (see section 4(d)). Calculations of splinter production for this case, even with generous assumptions, show that the riming–splintering mechanism was not rapid enough to explain the high concentrations of ice particles that were measured. These results support our original findings (Hobbs and Rangno 1985) and recent observations of Gayet and Soulage (1992), Vali (1992) and Takahashi (1993). On the other hand, on 20 August 1990, our calculations indicate (see section 4(f)) that the high ice particle concentrations could have originated from riming–splintering, but only if we assume that the non-columnar ice particles, which comprised a significant portion (30–50%) of the total ice particles, were also produced by riming–splintering. The virtual absence of precipitation-sized drops (>100 μm diameter) in these continental clouds indicates that neither rapid ice development nor ice enhancement depends on mechanisms that require supercooled drizzle or raindrops (e.g. Chisnell and Latham 1976; Lamb *et al.* 1981; Koenig 1984; Czys 1989).

In summary, the origin of ice in cumuliform clouds remains a mystery. However, the database we have presented here and elsewhere should be adequate for developing and testing proposed mechanisms.

Acknowledgement

This research was supported by a series of grants from the Division of Atmospheric Sciences of the US National Science Foundation, the latest of which is ATM-9015189. This paper was written while one of us (P.V.H.) was on study leave at Istituto FISBAT-CNR, Bologna, Italy.

References

Baker, B. A. 1991 On the role of phoresis in cloud ice initiation. *J. Atmos. Sci.*, **48**, 1545–1548

Battan, L. J. 1953 Observations of the formation and spread of precipitation in convective clouds. *J. Meteorol.*, **10**, 311–324

1963 Relationship between cloud base and initial radar echo. *J. Appl. Meteorol.*, **2**, 333–336

Baumgardner, D. and Spowart, M. 1990 Evaluation of the forward scattering spectrometer probe. Part III. Time response and laser inhomogeneity limitations. *J. Atmos. Technol.*, **7**, 666–672

Beard, K. V. 1992 Ice initiation in warm-base convective clouds: An assessment of microphysical mechanisms. *Atmos. Res.*, **28**, 125–152

Blanchard, D. C. 1957 The supercooling, freezing and melting of giant waterdrops at terminal velocity in air. Pp. 233–247 in *Artificial stimulation of rain*, Ed. H. Weickmann. Pergamon Press, New York

Chisnell, R. F. and Latham, J. 1976 Ice particle multiplication in cumulus clouds. *Q. J. R. Meteorol. Soc.*, **102**, 133–156

Czys, R. R. 1989 Ice initiation by collision-freezing in warm-based cumuli. *J. Appl. Meteorol.*, **28**, 1098–1104

Findeisen, W. 1942 Ergebnisse von Wolken-und Niederschlagsbeobactungen bei Wetterkundungesflugen uber See. Reichsamt f. Wetterdienst Forsch.u. Erfahrungsberichte, B., No. 8, 3–12

Fletcher, N. H. 1962 *The physics of rainclouds*. Cambridge University Press

Gayet, J.-F. and Soulage, R. G. 1992 Observation of high ice particle concentrations in convective cells and cloud glaciation evolution. *Q. J. R. Meteorol. Soc.*, **118**, 177–190

Gayet, J.-F., Brown, P. R. A. and Albers, F.	1993	A comparison of in-cloud measurements obtained with six PMS 2-DC probes. *J. Atmos. Ocean Technol.*, **10**, 180–194
Gokhale, N. R. and Spengler, J. D.	1972	Freezing of freely supercooled water drops by contact nucleation. *J. Appl. Meteorol.*, **11**, 157–160
Hallett, J. and Mossop, S. C.	1974	Production of secondary ice particles during the riming process. *Nature*, **249**, 26–28
Hobbs, P. V. and Rangno, A. L.	1985	Ice particle concentrations in cloud. *J. Atmos. Sci.*, **42**, 2523–2549
	1987	Reply to Telford *et al.*, *J. Atmos. Sci.*, **44**, 911–915
	1990a	Rapid development of ice particle concentrations in small polar maritime cumuliform clouds. *J. Atmos. Sci.*, **47**, 2710–2722
	1990b	'Summary of airborne data collected from the University of Washington's Convair C-131A research aircraft in maritime cumuliform clouds off and near the Washington State coast between 30 January 1987 and 14 March 1990'. (Available from the Cloud and Aerosol Research Group, University of Washington, Seattle, USA)
	1992	'Summary of airborne data collected from the University of Washington's Convair C-131A research aircraft in continental and semi-continental cumuliform clouds in Washington State between 27 April 1989 and 12 March 1992'. (Available from the Cloud and Aerosol Research Group, University of Washington, Seattle, USA)
Isaac, G. A.	1986	Summer cumulus cloud lifetime – important to static mode seeding. In *Precipitation enhancement – A scientific challenge. Meteorol. Monog.*, **21**, No. 43, 25–28
Knight, C. A., Hall, W. D. and Roskowski, R. M.	1983	Visual cloud histories related to first radar echo formation in northeast Colorado cumulus. *J. Clim. Appl. Meteorol.*, **22**, 1022–1040
Koenig, L. R.	1963	The glaciating behavior of small cumulonimbus clouds. *J. Atmos. Sci.*, **20**, 29–47
	1984	Further theoretical studies of the role of splintering in cumulus glaciation. *Q. J. R. Meteorol. Soc.*, **110**, 1121–1141
Lamb, D., Hallet, J. and Sax, R. I.	1981	Mechanistic limitations to the release of latent heat during the natural and artificial glaciation of deep convective clouds. *Q. J. R. Meteorol. Soc.*, **107**, 935–954
Ludlam, F. H.	1952	The production of showers by the growth of ice particles. *Q. J. R. Meteorol. Soc.*, **78**, 543–553
Mason, B. J.	1971	Pp. 251–279 in *The physics of clouds*. Oxford University Press
Meyers, M. P., DeMott, P. J. and Cotton, W. R.	1992	New primary ice-nucleation parameterizations in an explicit cloud model. *J. Appl. Meteorol.*, **31**, 708–721
Morris, T. R. and Braham Jr., R. R.	1968	'The occurrence of ice particles in Minnesota cumuli'. Pp. 306–315 in the Proceedings of the first national conference on weather modification, Albany. American Meteorological Society
Mossop, S. C.	1978	The influence of the drop size distribution in the production of secondary ice particles during graupel growth. *Q. J. R. Meteorol. Soc.*, **104**, 323–330
	1985a	The origin and concentration of ice crystals in clouds. *Bull. Am. Meteorol. Soc.*, **66**, 264–273
	1985b	Secondary ice particle production during rime growth: The effect of droplet size distribution and rimer velocity. *Q. J. R. Meteorol. Soc.*, **111**, 1113–1124
Mossop, S. C., Ono, A. and Wishart, E. R.	1970	Ice particles in maritime clouds near Tasmania. *Q. J. R. Meteorol. Soc.*, **96**, 487–508
Mossop, S. C., Cottis, R. E. and Bartlett, J. M.	1972	Ice crystal concentrations in cumulus and stratocumulous clouds. *Q. J. R. Meteorol. Soc.*, **98**, 105–126
Pitter, R. L. and Pruppacher, H. R.	1973	A wind tunnel investigation of freezing of small water drops falling at terminal velocity in air. *Q. J. R. Meteorol. Soc.*, **99**, 540–550
Politovich, M. K. and Cooper, W. A.	1988	Variability of the supersaturation in cumulus clouds. *J. Atmos. Sci.*, **45**, 1651–1664

Rangno, A. L. and Hobbs, P. V. 1983 Production of ice particles in clouds due to aircraft penetrations. *J. Clim. Appl. Meteorol.*, **22,** 214–232

1984 Further observations of the production of ice particles in clouds due to aircraft penetrations. *J. Clim. Appl. Meteorol.*, **23,** 985–987

1988 Criteria for the onset of significant concentrations of ice particles in cumulus clouds. *Atmos. Res.*, **22,** 1–13

1991 Ice particle concentrations and precipitation development and small polar maritime cumuliform clouds. *Q. J. R. Meteorol. Soc.*, **117,** 207–241

Raymond, D. J. and Blyth, A. M. 1989 Precipitation development in a New Mexico thunderstorm. *Q. J. R. Meteorol. Soc.*, **115,** 1397–1423

Rogers, D. P., Telford, J. W. and Chai, S. K. 1985 Entrainment and the temporal development of the microphysics of convective clouds. *J. Atmos. Sci.*, **42,** 1846–1858

Rosinski, J. 1991 Latent ice-forming nuclei in the Pacific Northwest. *Atmos. Res.*, **26,** 509–523

Sax, R. I., Eden, J. C. and Willis, P. T. 1976 'Single-level microphysical structure of Florida cumuli. Selected case studies'. Pp. 332–337 in Proceedings of the international cloud physics conference, Boulder

Schemenauer, R. S. and Isaac, G. A. 1984 The importance of cloud top lifetime in the description of natural cloud characteristics. *J. Clim. Appl. Meteorol.*, **23,** 267–279

Takahashi, T. 1993 High ice crystal production in winter cumuli over the Japan sea. *Geophys. Res. Lett.*, **20,** 451–454

Turner, F. M., Radke, L. F. and Hobbs, P. V. 1976 Optical techniques for counting ice particles in mixed phase clouds. *Atmos. Technol.*, **8,** 25–31

Vali, G. 1971 Quantitative evaluation of experimental results on the heterogeneous freezing nucleation of supercooled liquids. *J. Atmos. Sci.*, **28,** 402–409

1992 'Precipitation processes in mountain cumulus over the Asir region of Saudi Arabia'. Pp. 256–257 in Preprint 11th International conference on clouds and precipitation, Montreal, Canada

Willis, P. T. and Hallett, J. 1991 Microphysical measurements from an aircraft ascending with a growing isolated maritime cumulus tower. *J. Atmos. Sci.*, **48,** 283–300